

Conceptual understanding through efficient inverse-design of quantum optical experiments

Mario Krenn,^{1,2,*} Jakob Kottmann,¹ Nora Tischler,³ and Alán Aspuru-Guzik^{1,2,4,†}

¹*Department of Chemistry & Computer Science, University of Toronto, Canada.*

²*Vector Institute for Artificial Intelligence, Toronto, Canada.*

³*Centre for Quantum Dynamics, Griffith University, Brisbane, Australia.*

⁴*Canadian Institute for Advanced Research (CIFAR) Lebovic Fellow, Toronto, Canada*

(Dated: May 26, 2022)

The design of quantum experiments can be challenging for humans. This can be attributed at least in part to counterintuitive quantum phenomena such as superposition or entanglement. In experimental quantum optics, computational and artificial intelligence methods have therefore been introduced to solve the inverse-design problem, which aims to discover tailored quantum experiments with particular desired functionalities. While some computer-designed experiments have been successfully demonstrated in laboratories, these algorithms generally are slow, require a large amount of data or work for specific platforms that are difficult to generalize. Here we present THESEUS, an efficient algorithm for the design of quantum experiments, which we use to solve several open questions in experimental quantum optics. The algorithm's core is a physics-inspired, graph-theoretical representation of quantum states, which makes it significantly faster than previous comparable approaches. The gain in speed allows for topological optimization, leading to a reduction of the experiment to its conceptual core. Human scientists can therefore interpret, understand and generalize the solutions without performing any further calculations. We demonstrate THESEUS on the challenging tasks of generating and transforming high-dimensional, multi-photon quantum states. The final solutions are within reach of modern experimental laboratories, promising direct advances for empirical studies of fundamental questions, as well as technical applications such as quantum communication and photonic quantum information processing. In each case, the computer-designed experiment can be interpreted and conceptually understood. We argue that therefore, our algorithm contributes directly to the central aims of science.

Introduction – Photons, the quantum particles of light, are at the core of many quantum technologies that promise advances for imaging applications [1], efficient metrological schemes [2], fundamentally secure communication protocols [3] as well as simulation [4] and computation techniques [5–7] that are beyond the capabilities of their classical counterparts. Besides, photons are also among the core players in the experimental investigation of fundamental questions about the local and realistic nature of our universe.

Motivated by these opportunities, recent years have seen dramatic advances in quantum optical technology, which include highly complex operations in integrated photonic chips [8–12], generation of complex multiphotonic entanglement and its application [13–15], and the development and application of high-quality deterministic single-photon emitters [16] and highly efficient photon-number resolving detectors [17].

To advance technological and fundamental progress further and to enable the exploration of numerous proposed ideas in the laboratories, new experimental concepts and ideas are instrumental. Frequently, however, the design of experimental setups even for well-defined targets is challenging for the intuitions of

human experts, and existing systematic schemes (e.g. [18–20]) to date only provide solutions for specific experimental scenarios. For that reason, computational design methods for quantum optical experiments have been introduced [21], in the form of topological search augmented with machine learning [22, 23], genetic algorithms [24–26], active learning approaches [27], deep recurrent neural networks [28], and optimization of parametrized setups [29]. Unfortunately, due to the complexity and size of the Hilbert space as well as the breadth of quantum optical applications, those algorithms may have severe drawbacks, such as inefficient discovery rates, requirements of a huge amount of training data or specialization on narrow sets of problems. Most importantly, no method so far has shown how to systematically extract scientific ideas, concepts and understanding from the solutions of the computer algorithm.

Here we demonstrate THESEUS, an inverse-design algorithm for quantum optics based on a physics-inspired representation in the form of weighted graphs. THESEUS is generally applicable to discrete-variable quantum optics problems (including post-selected and non-postselected states, probabilistic and deterministic photon sources), does not need training data, and is orders of magnitude faster than previous comparable approaches. The speed-up allows for the application of topological optimization, which uncovers the conceptual cores underlying the solution. Physicists can then interpret, understand and generalize those

* mario.krenn@utoronto.ca

† alan@aspuru.com

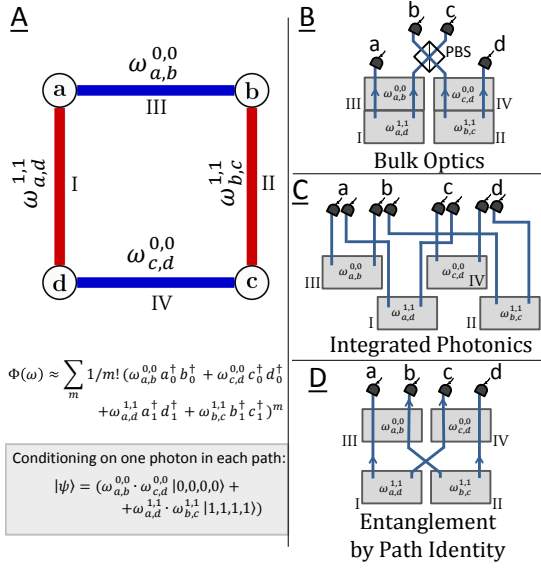


Figure 1. A weighted edge-coloured graph as an abstract and efficient representation of the quantum information of a large variety of quantum optics experiments. **A**: As a specific example, we show a graph with four vertices and four coloured and weighted edges. The vertices $a - d$ correspond to photonic paths, the edges correspond to correlated photon pairs, the edge colours stand for mode numbers, and weights $\omega \in \mathbb{C}$ stand for complex coefficients. Probabilistic sources create the photon pairs (edges). Thus the entire information about the quantum state is represented by $\Phi(\omega)$, with x_k^\dagger being a creation operator of a photon in path x with mode number k . The information carried in the graph can be translated to different schemes of quantum optical experiments, such as **(B)** Entanglement by Path Identity, **(C)** standard bulk optics, for example with polarisation as the carrier of quantum information, or **(D)** path encodings. The results of the quantum experiments can directly be calculated from the information of the graph. For example, a prominent technique is to condition the state on obtaining a click in each of the four detectors (post-selection). The equivalent formulation in terms of graphs is the sum of all subsets of edges that contain every vertex exactly once. It reduces the example quantum state to two terms. If all weights are equal, the resulting quantum state is a four-qubit GHZ state. Access to $\Phi(\omega)$ allows for the optimisation of non-postselected, heralded and triggered quantum states too, as we show in examples within the manuscript.

instances. We demonstrate THESEUS on several questions about experiments that previously had no (feasible) solution. Concretely, we investigate complex multiphotonic entanglement, the generation of heralded entanglement and complex photonic quantum transformations. In all of these cases, we uncover previously unknown generalizable patterns and new experimental ideas and interpretations.

Graph Theory–Quantum Experiment Mapping – We utilize and expand a recent connection that shows how coloured graphs can represent the essential

information of quantum optical experiments involving probabilistic photon-pair sources [30] and linear optical components [31]. The key idea (explained in Fig.1) is that a weighted coloured graph encodes the entire information produced by a photonic quantum experiment. The vertices correspond to spatial photon paths and edges between vertex v_1 and v_2 stand for probabilistic photon pairs in path v_1 and v_2 . The edge colour represents the internal mode number of the photons and edge weights ω stand for amplitudes.

The extension we present here gives access to the complete information of quantum optical experiments through a weight function $\Phi(\omega)$ (rather than only post-selected states, as in [30–32]), and allows us to generalize the scope of the method significantly. It allows for the description of non-postselected states, triggered and heralded photonic states, states with multiple excitations per mode (such as NOON states [33]) and general quantum transformations. Furthermore, it enables the description of photon-number sensitive and insensitive detectors (which correspond to different projections of $\Phi(\omega)$) and deterministic photon sources such as quantum dots (see SI for details).

Furthermore, we present here that graphs can be directly translated to several different schemes of photonic quantum optics, such as standard bulk optics, integrated photonics or entanglement by path identity [34, 35]. A given graph can be translated in multiple ways to quantum experimental setups, while each setup corresponds to precisely one graph (more details in SI). These extensions were necessary to use the graph-theoretical description as a tool for the inverse-design of quantum experiments that are feasible in state-of-the-art quantum photonics laboratories.

Graph-based inverse-design of Quantum Experiments – The abstract and general representation of quantum experiments as graphs allows us to find a new method for inverse-designing quantum experiments. The idea is to write an optimisation objective function in terms of weights ω of the graph.

The most general quantum state corresponds to a complete graph with all possible multi-coloured weighted edges between each vertex (see Fig.2). As an essential step, we need to construct the state fidelity in terms of weights, $F(\omega)$. While the entire quantum state $\Phi(\omega)$ is directly defined from the edge weights, conditioning measurements are commonly used to obtain more intricate states and to overcome the lack of single-photon nonlinearities. Prominent examples for such measurements are conditioning on the simultaneous detection of one photon in each path (I), conditioning on the detection of ancilla photons (II), or combinations thereof.

As an example, we show the construction of the fidelity for a 4-photon GHZ state $|GHZ\rangle = 1/\sqrt{2}(|0,0,0,0\rangle + |1,1,1,1\rangle)_{a-d}$, where $|0\rangle$ and $|1\rangle$ stand for one photon in the internal mode 0 and 1 (such as horizontal or vertical polarisation), respec-

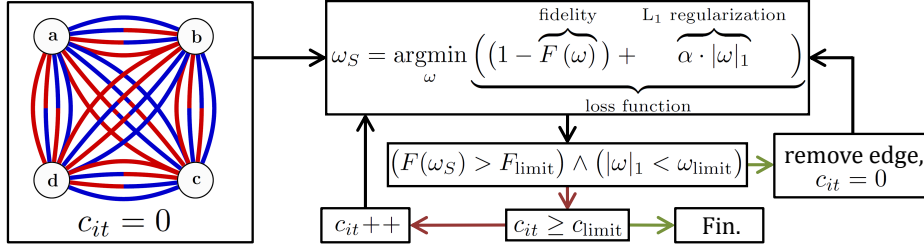


Figure 2. **Algorithm – THESEUS:** The initial graph contains all possible edges between each vertex, leading to $|G| = d^2 \frac{n(n-1)}{2}$ edges (with n vertices and d different edge colors), each of them having an independent complex weight $\omega_{v_1, v_2}^{m_1, m_2}$. The main step is a minimization of the loss function, which contains the quantum fidelity in terms of weights of the graph. Additionally, an L_1 regularization term controls the magnitude of the weights. If the weights identified by the optimisation, ω_S , lead to fidelities larger than a F_{limit} , and the magnitude of the weights is smaller than ω_{limit} , then one edge of the graph is removed, and the optimisation continues with the smaller graph. On the other hand, if the criteria are not fulfilled, the same graph is optimised (with different starting conditions) until the discovery of a suitable solution, or the number of iterations exceeds c_{limit} . The result of THESEUS is a weighted graph that leads to sufficiently large fidelities, with a small number of edges. This topological optimisation enables the scientific interpretation and understanding of results.

tively. The subscript $a-d$ means one photon is in each of the four paths a, b, c and d . Under the condition of simultaneous detection (I), the term $|0, 0, 0, 0\rangle$ can be generated by three different subgraphs: two blue horizontal edges, vertical edges or crossed edges. The weight of a subgraph is the product of all its edge weights. The weight of the whole term is the sum of all weights of the subgraphs. Therefore, the weight of $|0, 0, 0, 0\rangle$ is

$$\omega_{|0,0,0,0\rangle} = \omega_{a,b}^{0,0} \omega_{c,d}^{0,0} + \omega_{a,c}^{0,0} \omega_{b,d}^{0,0} + \omega_{a,d}^{0,0} \omega_{b,c}^{0,0} \quad (1)$$

In an equivalent way, the amplitude of $|1, 1, 1, 1\rangle$ can be written in terms of ω . As a result, we have

$$F(\omega) = \frac{|\omega_{|0,0,0,0\rangle} + \omega_{|1,1,1,1\rangle}|^2}{2 \cdot N(\omega)^2} \quad (2)$$

where $N(\omega)$ is a normalisation constant of the state emerging from the graph (more details in SI).

The weights of the graph are optimised by minimising a loss function constructed from the fidelity and an additional L_1 regularisation term

$$L(\omega) = (1 - F(\omega)) + \alpha \cdot |\omega|_1 \quad (3)$$

with positive real coefficient $\alpha < 1$. Inclusion of the L_1 regularization term can drive the optimisation towards a solution with smaller amplitudes, thereby opening ways to further reduce the edges of the graph by removing edges with small weights. For optimisation, we use the Broyden-Fletcher-Goldfarb-Shanno algorithm, an iterative quasi-Newton method to solve non-linear optimisation problems. If we identify a solution with $F(\omega)$ above a limit (we use $F_{\text{limit}} = 0.95$) and small weights ω (we use $\omega_{\text{limit}} = 1$), we found a

suitable experimental setup candidate. At this point, as the loss minimization is fast, we can perform a topological optimisation. We reduce the size of the graph by iteratively removing individual edges. We can choose the edge from a distribution that depends on the magnitude of the weights of the previous solution (with two special cases: choosing entirely randomly, and always choosing the edge with the smallest weight magnitude). The new, smaller graph will be used to minimize the loss function in eq.(3). The topological optimisation reduces the size of the graph iteratively.

While topological optimisation is computationally more intense than optimising for a set of weight parameters, it is essential for successful interpretations and scientific understanding of the solution. As we show in examples below, the topological optimisation distills small structures such that human scientists can interpret and understand the underlying physical principles, and use the new knowledge to solve other cases. In many instances, we used the initial insight from the topological optimisation to find a straightforward generalization of the new concept to infinitely large classes of situations. This is in stark contrast to typical artificial intelligence applications in the natural sciences [36], where the solution of a parameter optimisation is the final product, without the intention of discovering new scientific ideas (with few recent exceptions that investigate toy-examples [37]).

Benchmarking – We compare the speed of THESEUS with previous comparable approaches, using classes of high-dimensional multipartite states called Schmidt-Rank Vectors (SRV) as a benchmark [38]. In particular, we aim to discover maximally entangled three-party quantum states of up to ten local dimensions. This task is well understood theoretically, thus it represents a good benchmark. There are 81 unique entangled structures that could be generated using lin-

ear optics [32]. A pure topological circuit search using 50.000 CPU-hours has discovered 51 out of 81 different states in the set [22]. A reinforcement learning algorithm has identified 17 out of 81 different states, with speed comparable to the topological search algorithm [27]. THESEUS discovers 76 different states within 2 hours, where the first 17 are identified within two seconds, and the first 51 states in less than 15 minutes.

We turn to a second benchmarking task; the identification of high-dimensional CNOT gates. A recent study has shown that the identification of the first photonic high-dimensional controlled operation took 150.000 CPU-hours [39]. Our algorithm finds a solution that is experimentally quantitatively simpler, within 1 CPU-second. We come back to this example in Fig.5.

Scientific Discovery and Understanding – The improvement in speed shows that THESEUS is ready to go beyond benchmarks, and be applied to the discovery of new scientific targets and – more importantly – to the development of new scientific insights

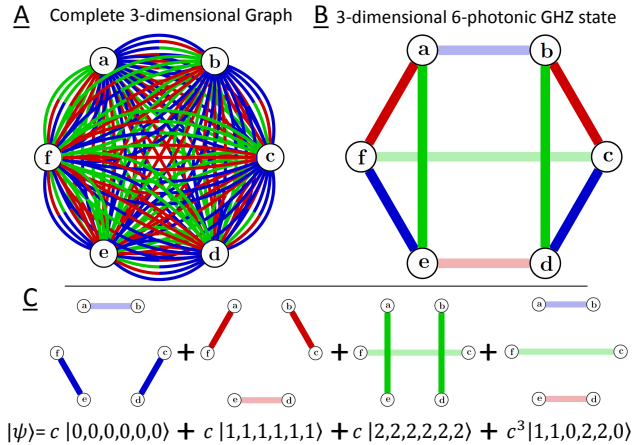


Figure 3. Finding a 3-dimensional 6-photonic GHZ state. **A:** The complete graph of six vertices and three colours is the initial state. Each pair of vertices is connected by nine edges, which stand for all nine possibilities (blue, red, green stands for modes 0,1,2, respectively). A bi-coloured edge stands for a photon pair with different mode numbers. For example, a blue-red edge between vertex a and b stands for a photon pair with one photon in path a with mode number 0, and one photon in b with mode number 1, i.e. $a_0^\dagger b_1^\dagger$. In total, this corresponds to 135 edges. **B:** The solution for a 6-photonic 3-dimensional GHZ state. While it has been shown that such a state cannot be created with perfect fidelity [30] with linear optics and probabilistic photon-pair sources (without additional photons), THESEUS found a solution where the fidelity scales with $F \approx 1 - O(c^4)$ with the overall counts C scaling as $C \approx O(c^2)$, which is experimentally feasible. **A:** The concept of the solution can be interpreted in the context of graph-theoretical results and can be immediately generalized by human scientists.

and understanding. Scientific understanding is essential to the epistemic aims of science [40], but rarely addressed in applications of artificial intelligence to the natural sciences. In the philosophy science, pragmatic criteria have been found for *scientific understanding*, in particular by de Regt’s award-winning work [40, 41]. He describes that scientists can understand a phenomenon *if they can recognise qualitatively characteristic consequences without performing exact calculations*. We connect this criterion to our discoveries: We discover the first high-dimensional six-photonic GHZ states, which have been conjectured to be not constructible with linear optics. We can understand the underlying concept and use it to construct a simple method to generate high-dimensional GHZ states with an arbitrary number of photons. Furthermore, we discover the first solutions of heralded three-dimensional Bell states and understand the underlying concept which we generalise to arbitrary-dimensional Bell states – without additional calculations. Similarly, we discover setups for heralded GHZ states that need fewer resources than methods proposed in the literature. We furthermore apply THESEUS on multiphotonic transformations. We find a new way to interpret and construct photonic qubit operations such as CNOT or TOFFOLI gates. Similarly, we discover high-dimensional CNOT operations that need quantitatively less resources than methods proposed in the literature. Connecting to de Regt’s criterion, we see that our algorithm has been the source of scientific understanding for multiple instances.

High-dimensional GHZ states – A d -dimensional n -partite GHZ quantum state is written as

$$|\psi\rangle = \frac{1}{\sqrt{d}} \sum_{i=0}^{d-1} |\underbrace{i, i, i, \dots}_{n \text{ times}}\rangle. \quad (4)$$

These states are studied in the interplay between quantum and local-realistic theories [42–45], and have recently found potential applications in quantum communication tasks [46].

Graph-theoretical arguments show that perfect high-dimensional GHZ states can be generated only for 4-photon states [30, 47], because terms in addition to those in eq.(9) necessarily emerge. Using THESEUS, we discover the first example that circumvents the no-go theorem, see Fig.3. The algorithm identifies solutions with fidelities arbitrarily close to one, by adjusting the edge weights in such a way that unwanted terms have arbitrarily small weights (albeit at the expense of lower count rates). Upon interpreting this solution, it can be immediately generalized to GHZ states with higher dimensions and a larger number of particles. The idea is to start with a cycle graph and add $(d - 2)$ perfect matchings (a perfect matching is a set of edges that contain every vertex exactly once), with all edge weights being equal. The weights

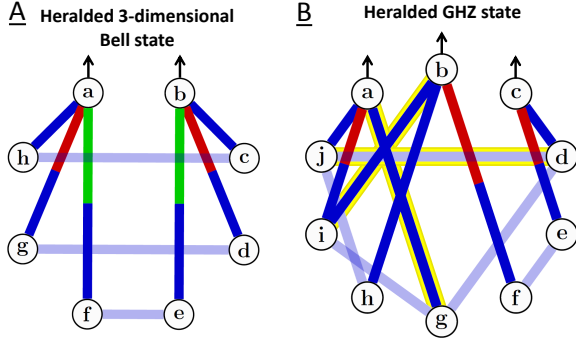


Figure 4. **Heralded entangled states.** **A:** Solution for a heralded 3-dimensionally entangled Bell state. Solutions for 2-dimensional Bell states have been reported, their generalisation to higher dimensions is so far missing. The solution can immediately be understood: The algorithm connected each edge from an outgoing photon (in path a and b) to one individual trigger photon (vertices $c-h$), and connected the triggers with the same colour with a low-weighted edge. This solution can immediately be generalised to arbitrary high-dimensional Bell states. **B:** Solution for a heralded GHZ state. It is closely related to the concept discovered in (A), where each colored edge in the output photons (in path a , b and c) is connected to an individual trigger vertex. This solution however produces one additional term, which is destructively interfered by adding three extra edges (marked in yellow). The concept can be clearly interpreted and generalised, see SI.

of all edges that occur in more than one subgraph are multiplied with a constant $c < 1$, which controls the fidelity. No further computations or optimisations are necessary, demonstrating that we achieved *scientific understanding* based on a computational optimisation in the appropriate representation of the problem at hand.

Heralded photonic entangled states – The next targets we address are heralded entangled photonic states. Standard sources of photonic entanglement such as spontaneous parametric down-conversion or spontaneous four-wave mixing, are entirely probabilistic [9, 48]. That means photons are produced at random times, and only after the detection of the photon state, one knows that they have been created. The generation of heralded states would allow for event-ready schemes, which are essential in photonic quantum computation [49, 50] and quantum communication [51]. Experimentally, two-dimensional Bell states have been generated using four ancilla photons [52, 53]. Implementation ideas for higher-dimensional generalizations of heralded Bell states [54] have been missing so far. We target the identification of a heralded 3-dimensional Bell state, and within seconds, we find a solution, see Fig.4A. The setup requires four SPDC events simultaneously, which is well within today’s experimental capabilities [55–57]. We identify a remarkable structure: Each edge from the output

photons a and b is connected to an individual ancilla vertex, with additional edges between horizontal vertices. This structure ensures that whenever the heralding photons are detected, an approximate Bell state is generated in a and b with fidelities arbitrarily close to one. The structure can immediately be generalized to arbitrary higher dimensions, demonstrating once more computer-inspired scientific understanding.

Theoretical schemes for the production of multi-photon entangled GHZ states have been proposed a decade ago, but never experimentally implemented due to their experimental requirements [58, 59]. Such states, however, provide the resources for definite demonstration of deterministic violations of local-realistic worldviews [60]. We find an experimental configuration, which requires fewer resources and which is within reach of experimental capabilities, see Fig.4B. The discovered concept is strongly related to the bipartite case, in the sense that it connects each edge of the output modes $a-c$ to an individual vertex. In addition, it contains three edges that lead to the destructive interference of one additional term in the quantum state. We explain the details and generalizations in the SI.

Photonic Controlled-Gates – Finally, we demonstrate the usage of THESEUS to photonic quantum transformations, which are essential elements for photonic quantum simulation [4] and computation schemes [17, 61–64]. To this end, we introduce two new ideas. First, we need to simultaneously optimise $d_{\text{trafo}} = d_C \cdot d_T$ graphs, where d_C and d_T stand for the dimension of the control and target photon, respectively. Each graph stands for the transformation of one $|C, T\rangle$ setting. As all graphs represent one single experimental setup, edges between the output modes (a, b) and trigger modes (denoted by lowercase letters c, d, e, \dots) have to stay the same for all d_{trafo} graphs. Second, virtual vertices V_a and V_b stand for incoming photons. Edges between a virtual vertex and $a-d$ (in all d_{trafo} graphs together) represent a unitary transformation of the incoming photon. The control (target) photon has d_C (d_T) internal modes represented by the different colors of edges connected to the virtual vertex V_a (V_b). The new fidelity function is the average of all d_{trafo} fidelities of all individual graphs. Each individual graph can be interpreted as a state generation. Therefore, the entire state transformation can be understood as d_{trafo} state generations, which are strongly interdependent.

As a first example, we demonstrate a two-qubit CNOT operation ($d_C = d_T = 2$). Here, experimental setups are well studied, both theoretically and experimentally [65–68]. We start the optimisation from the most general four graphs possible, with the restrictions as described above (more details in SI). In Fig.5, we show the resulting four graphs, which provide a CNOT operation. We find an understandable underlying concept, which has not been discussed be-

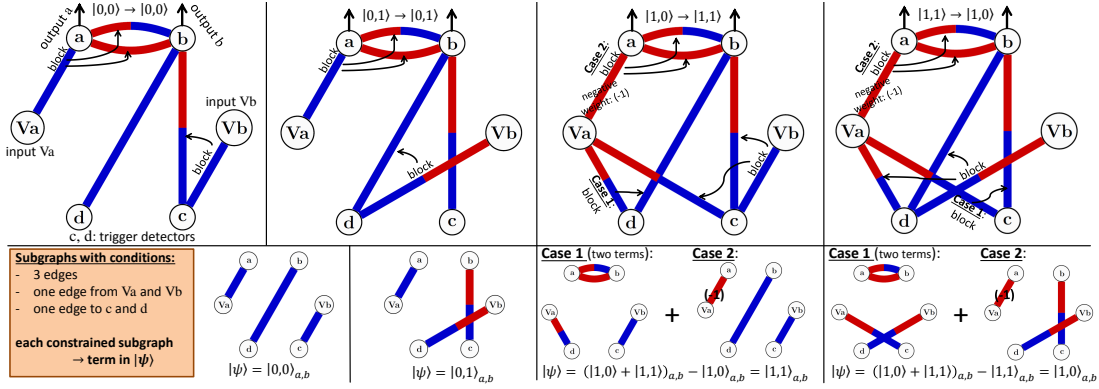


Figure 5. **Qubit CNOT Transformation:** Two input photons (denoted as Va and Vb) undergo a CNOT operation, and output in path a and b, conditioned on the simultaneous detection of one photon in each of the trigger paths c and d. This example goes beyond state generation and shows how the same framework allows identification of quantum transformations. We introduce *virtual* vertices Va and Vb, which are interpreted as incoming photons. Edges between a virtual vertex and vertices a-d (in all graphs together) represent unitary transformations of the incoming photon. For example, if $Vb=|0\rangle$, the photon goes to path c, while for $Vb=|1\rangle$ it goes to path d. The CNOT consists of four individual transformations (one for each of the inputs $|0,0\rangle, |0,1\rangle, |1,0\rangle, |1,1\rangle$). Each transformation stands for one graph and the subgraph of vertices a-d has to stay constant for each transformation. The four graphs in the upper row are the solution of an inverse-design for a two-qubit CNOT. The quantum state in the output of a,b (after conditioning on the trigger detectors c,d) is governed by all subgraphs that fulfil the following conditions (see orange inset): Contains three edges (two edges from incoming photons, and one ancillary photon pair); each of the virtual vertices Va and Vb is contained in one edge (that symbolizes that one photon is entering the setup), and both c and d are contained in an edge (such that the two triggers detect a photon in path c and d). The solution can be conveniently interpreted: No vertex can have two incoming edges (as follows from the three conditions). Therefore, an edge involving Va or Vb block all edges at the other vertex of the edge, which significantly simplifies the interpretation of the graphs. The resulting terms are written in the lower row. From the solution, we discover an interesting concept: If $Va=|0\rangle$, the edge involving Vb *chooses* the outgoing term by blocking the appropriate edge. However, if $Va=|1\rangle$, the double edge between a and b is active – as the weight $\omega_{Va,a}^{1,1} = (-1)$, Vb chooses the term that will destructively interfere. The idea of having one virtual vertex choosing the terms can be generalized to more complex multi-qubit transformations.

fore in the scientific literature. The idea is to prepare the circuit in such a way that the vertex for the incoming target photon “chooses” which state will be generated. That is possible if the resulting subgraphs for $C = 0$ appear also for the case $C = 1$, but with a negative weight (see Case2 for $C = 1$ in Fig.5). In the case $C = 1$, one can add two terms in the output, and destructive interference will eliminate the wrong term. Interestingly, exactly this concept has been the core of one of the first photonic CNOT experiments [67], which gives a new interpretation for a 16-year-old experiment (see SI for details). The concept can be immediately generalized to multi-qubit transformations.

We apply THESEUS to the discovery of high-dimensional quantum transformations, which have been discussed in the context of resource-efficient quantum computation algorithms [69–71]. Only recently, the first experimental proposals for multi-level transformations have been discovered [39]. We specifically search for a system with $d_C = 2$ and $d_T = 3$. We identify a solution that is experimentally much simpler than previous methods [39]. It requires four ancillary photons and two input/output photons (six photons in total), which is within reach of current multi-photon and multi-level quantum experiments [14, 15, 72–74].

The solution can be understood as a combination of the 2-dimensional CNOT in Fig.5, and the reduction of weights as described in Fig. 3 (full details of the setups in SI).

Conclusion – We presented the algorithm THESEUS for the inverse-design of quantum optical experiments, which is based on an abstract physics-inspired representation. We use it to discover several previously unknown experimental configurations of quantum states and transformations in the challenging high-dimensional and multi-photon regime. Those experimental concepts are within reach of modern photonic technology and could lead to fascinating experimental investigations of fundamental questions and technological advances. THESEUS can immediately be applied to discover a multitude of other targets in experimental quantum optics, such as tools to enable silicon-photonics quantum computation [63], highly efficient, low-noise quantum entanglement sources [55], applications in quantum metrology [2] or in quantum-enhanced microscopes and telescopes [75, 76]

One of the main features is the possibility to extract scientific understanding from the computer-inspired designs. That was made possible by a topological optimisation that reduces the solutions to fundamental

building blocks. Those minimal topologies allow for the interpretation and generalizations of the discovered solution, without performing additional calculations. This is in accord with criteria from the philosophy of science that argue that scientific understanding is connected with the skill to use concepts fruitfully, *without exact calculations*. Hence, in a broader sense, we argue that the ability of our algorithm goes beyond simple optimisation, and enters the realm of providing scientific insights and allowing for scientific understanding. Thereby, it directly contributes to the essential aim of science.

ACKNOWLEDGEMENTS

This work was supported by the Google Focused Award on Quantum Computing, the Industrial Re-

search Chair Program of Canada and by the U.S. Department of Energy, Office of Science, Office of Advanced Scientific Computing Research, Quantum Algorithm Teams Program. A. A.-G. acknowledges generous support from the Canada 150 Research Chair Program, Tata Steel, Anders G. Frøseth, and the Office of Naval Research. M.K. acknowledges support from the Austrian Science Fund (FWF) through the Erwin Schrödinger fellowship No. J4309. N.T. acknowledges support by the Griffith University Postdoctoral Fellowship Scheme.

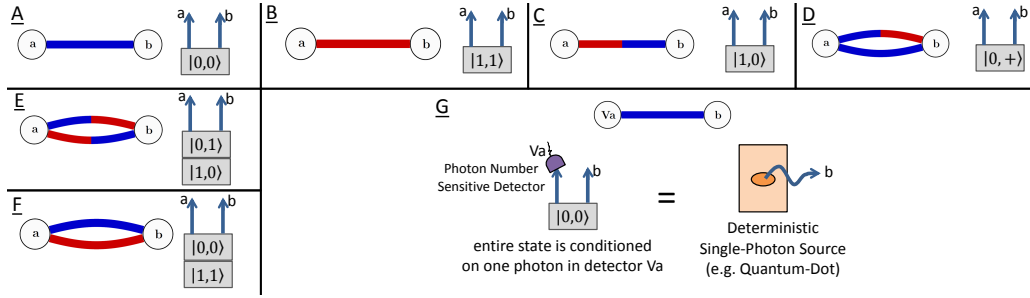
-
- [1] P.A. Moreau, E. Toninelli, T. Gregory and M.J. Padgett, Imaging with quantum states of light. *Nature Reviews Physics* **1**, 367–380 (2019).
 - [2] E. Polino, M. Valeri, N. Spagnolo and F. Sciarrino, Photonic Quantum Metrology. *arXiv:2003.05821* (2020).
 - [3] N. Gisin and R. Thew, Quantum communication. *Nature Photonics* **1**, 165 (2007).
 - [4] A. Aspuru-Guzik and P. Walther, Photonic quantum simulators. *Nature Physics* **8**, 285–291 (2012).
 - [5] S. Aaronson and A. Arkhipov, The computational complexity of linear optics. *Proceedings of the forty-third annual ACM symposium on Theory of computing* 333–342 (2011).
 - [6] A. Peruzzo, J. McClean, P. Shadbolt, M.H. Yung, X.Q. Zhou, P.J. Love, A. Aspuru-Guzik and J.L. O’Brien, A variational eigenvalue solver on a photonic quantum processor. *Nature Communications* **5**, 4213 (2014).
 - [7] M. Gimeno-Segovia, P. Shadbolt, D.E. Browne and T. Rudolph, From three-photon Greenberger-Horne-Zeilinger states to ballistic universal quantum computation. *Physical Review Letters* **115**, 020502 (2015).
 - [8] J. Carolan, C. Harrold, C. Sparrow, E. Martín-López, N.J. Russell, J.W. Silverstone, P.J. Shadbolt, N. Matsuda, M. Oguma, M. Itoh and others, Universal linear optics. *Science* **349**, 711–716 (2015).
 - [9] J. Wang, F. Sciarrino, A. Laing and M.G. Thompson, Integrated photonic quantum technologies. *Nature Photonics* **14**, 273–284 (2020).
 - [10] L.T. Feng, G.C. Guo and X.F. Ren, Progress on Integrated Quantum Photonic Sources with Silicon. *Advanced Quantum Technologies* **44**, 1277–1280 (2019).
 - [11] D. Llewellyn, Y. Ding, I.I. Faruque, S. Paesani, D. Bacco, R. Santagati, Y.J. Qian, Y. Li, Y.F. Xiao, M. Huber and others, Chip-to-chip quantum teleportation and multi-photon entanglement in silicon. *Nature Physics* **16**, 148–153 (2020).
 - [12] L. Lu, L. Xia, Z. Chen, L. Chen, T. Yu, T. Tao, W. Ma, Y. Pan, X. Cai, Y. Lu and others, Three-dimensional entanglement on a silicon chip. *npj Quantum Information* **6**, 1–9 (2020).
 - [13] H. Rubinsztein-Dunlop, A. Forbes, M.V. Berry, M.R. Dennis, D.L. Andrews, M. Mansuripur, C. Denz, C. Alpmann, P. Banzer, T. Bauer and others, Roadmap on structured light. *Journal of Optics* **19**, 013001 (2016).
 - [14] X.L. Wang, Y.H. Luo, H.L. Huang, M.C. Chen, Z.E. Su, C. Liu, C. Chen, W. Li, Y.Q. Fang, X. Jiang and others, 18-qubit entanglement with six photons’ three degrees of freedom. *Physical Review Letters* **120**, 260502 (2018).
 - [15] Y.H. Luo, H.S. Zhong, M. Erhard, X.L. Wang, L.C. Peng, M. Krenn, X. Jiang, L. Li, N.L. Liu, C.Y. Lu and others, Quantum teleportation in high dimensions. *Physical Review Letters* **123**, 070505 (2019).
 - [16] H. Wang, Y. He, Y.H. Li, Z.E. Su, B. Li, H.L. Huang, X. Ding, M.C. Chen, C. Liu, J. Qin and others, High-efficiency multiphoton boson sampling. *Nature Photonics* **11**, 361–365 (2017).
 - [17] S. Slussarenko and G.J. Pryde, Photonic quantum information processing: A concise review. *Applied Physics Reviews* **6**, 041303 (2019).
 - [18] N. VanMeter, P. Lougovski, D. Uskov, K. Kieling, J. Eisert and J.P. Dowling, General linear-optical quantum state generation scheme: applications to maximally path-entangled states. *Physical Review A* **76**, 063808 (2007).
 - [19] F. Shahandeh, A.P. Lund, T.C. Ralph and M.R. Vanner, Arbitrary multi-qubit generation. *New Journal of Physics* **18**, 103020 (2016).
 - [20] N. Tischler, C. Rockstuhl and K. Słowik, Quantum optical realization of arbitrary linear transformations allowing for loss and gain. *Physical Review X* **8**, 021017 (2018).
 - [21] M. Krenn, M. Erhard and A. Zeilinger, Computer-inspired Quantum Experiments. *arXiv:2002.09970* (2020).
 - [22] M. Krenn, M. Malik, R. Fickler, R. Lapkiewicz and A. Zeilinger, Automated search for new quantum exper-

- iments. *Physical Review Letters* **116**, 090405 (2016).
- [23] X. Zhan, K. Wang, L. Xiao, Z. Bian, Y. Zhang, B.C. Sanders, C. Zhang and P. Xue, Experimental quantum cloning in a pseudo-unitary system. *Physical Review A* **101**, 010302 (2020).
- [24] P. Knott, A search algorithm for quantum state engineering and metrology. *New Journal of Physics* **18**, 073033 (2016).
- [25] L. O'Driscoll, R. Nichols and P. Knott, A hybrid machine learning algorithm for designing quantum experiments. *Quantum Machine Intelligence* **1**, 5–15 (2019).
- [26] R. Nichols, L. Mineh, J. Rubio, J.C. Matthews and P.A. Knott, Designing quantum experiments with a genetic algorithm. *Quantum Science and Technology* **4**, 045012 (2019).
- [27] A.A. Melnikov, H.P. Nautrup, M. Krenn, V. Dunjko, M. Tiersch, A. Zeilinger and H.J. Briegel, Active learning machine learns to create new quantum experiments. *Proceedings of the National Academy of Sciences* **115**, 1221–1226 (2018).
- [28] T. Adler, M. Erhard, M. Krenn, J. Brandstetter, J. Kofler and S. Hochreiter, Quantum optical experiments modeled by Long Short-Term Memory. *arXiv:1910.13804* (2019).
- [29] J.M. Arrazola, T.R. Bromley, J. Izaac, C.R. Myers, K. Brádler and N. Killoran, Machine learning method for state preparation and gate synthesis on photonic quantum computers. *Quantum Science and Technology* **4**, 024004 (2019).
- [30] M. Krenn, X. Gu and A. Zeilinger, Quantum experiments and graphs: Multiparty states as coherent superpositions of perfect matchings. *Physical Review Letters* **119**, 240403 (2017).
- [31] X. Gu, M. Erhard, A. Zeilinger and M. Krenn, Quantum experiments and graphs II: Quantum interference, computation, and state generation. *Proceedings of the National Academy of Sciences* **116**, 4147–4155 (2019).
- [32] X. Gu, L. Chen, A. Zeilinger and M. Krenn, Quantum experiments and graphs. III. High-dimensional and multiparticle entanglement. *Physical Review A* **99**, 032338 (2019).
- [33] I. Afek, O. Ambar and Y. Silberberg, High-NOON states by mixing quantum and classical light. *Science* **328**, 879–881 (2010).
- [34] M. Krenn, A. Hochrainer, M. Lahiri and A. Zeilinger, Entanglement by path identity. *Physical Review Letters* **118**, 080401 (2017).
- [35] J. Kysela, M. Erhard, A. Hochrainer, M. Krenn and A. Zeilinger, Experimental High-Dimensional Entanglement by Path Identity. *arXiv:1904.07851* (2019).
- [36] G. Carleo, I. Cirac, K. Cranmer, L. Daudet, M. Schuld, N. Tishby, L. Vogt-Maranto and L. Zdeborová, Machine learning and the physical sciences. *Reviews of Modern Physics* **91**, 045002 (2019).
- [37] R. Iten, T. Metger, H. Wilming, L. Del Rio and R. Renner, Discovering physical concepts with neural networks. *Physical Review Letters* **124**, 010508 (2020).
- [38] M. Huber and J.I. Vicente, Structure of multidimensional entanglement in multipartite systems. *Physical Review Letters* **110**, 030501 (2013).
- [39] X. Gao, M. Erhard, A. Zeilinger and M. Krenn, Computer-inspired concept for high-dimensional multipartite quantum gates. *arXiv:1910.05677* (2019).
- [40] H.W. De Regt and D. Dieks, A contextual approach to scientific understanding. *Synthese* **144**, 137–170 (2005).
- [41] H.W. De Regt, Understanding scientific understanding. *Oxford University Press* (2017).
- [42] J. Ryu, C. Lee, M. Żukowski and J. Lee, Greenberger-Horne-Zeilinger theorem for N qudits. *Physical Review A* **88**, 042101 (2013).
- [43] J. Lawrence, Rotational covariance and Greenberger-Horne-Zeilinger theorems for three or more particles of any dimension. *Physical Review A* **89**, 012105 (2014).
- [44] W. Tang, S. Yu and C. Oh, Multisetting Greenberger-Horne-Zeilinger paradoxes. *Physical Review A* **95**, 012131 (2017).
- [45] M. Erhard, M. Malik, M. Krenn and A. Zeilinger, Experimental Greenberger-Horne-Zeilinger entanglement beyond qubits. *Nature Photonics* **12**, 759–764 (2018).
- [46] M. Pivoluska, M. Huber and M. Malik, Layered quantum key distribution. *Physical Review A* **97**, 032312 (2018).
- [47] I. Bogdanov, Graphs with only disjoint perfect matchings. *MathOverflow* <https://mathoverflow.net/q/267013> (2017).
- [48] J.W. Pan, Z.B. Chen, C.Y. Lu, H. Weinfurter, A. Zeilinger and M. Żukowski, Multiphoton entanglement and interferometry. *Reviews of Modern Physics* **84**, 777 (2012).
- [49] D.E. Browne and T. Rudolph, Resource-efficient linear optical quantum computation. *Physical Review Letters* **95**, 010501 (2005).
- [50] P. Kok, W.J. Munro, K. Nemoto, T.C. Ralph, J.P. Dowling and G.J. Milburn, Linear optical quantum computing with photonic qubits. *Reviews of Modern Physics* **79**, 135 (2007).
- [51] S.H. Tan and P.P. Rohde, The resurgence of the linear optics quantum interferometer - recent advances & applications. *Reviews in Physics* 100030 (2019).
- [52] S. Barz, G. Cronenberg, A. Zeilinger and P. Walther, Heralded generation of entangled photon pairs. *Nature Photonics* **4**, 553 (2010).
- [53] C. Wagenknecht, C.M. Li, A. Reingruber, X.H. Bao, A. Goebel, Y.A. Chen, Q. Zhang, K. Chen and J.W. Pan, Experimental demonstration of a heralded entanglement source. *Nature Photonics* **4**, 549 (2010).
- [54] D. Sych and G. Leuchs, A complete basis of generalized Bell states. *New Journal of Physics* **11**, 013006 (2009).
- [55] H.S. Zhong, Y. Li, W. Li, L.C. Peng, Z.E. Su, Y. Hu, Y.M. He, X. Ding, W. Zhang, H. Li and others, 12-photon entanglement and scalable scattershot boson sampling with optimal entangled-photon pairs from parametric down-conversion. *Physical Review Letters* **121**, 250505 (2018).
- [56] X.L. Wang, L.K. Chen, W. Li, H.L. Huang, C. Liu, C. Chen, Y.H. Luo, Z.E. Su, D. Wu, Z.D. Li and others, Experimental ten-photon entanglement. *Physical Review Letters* **117**, 210502 (2016).
- [57] L.K. Chen, Z.D. Li, X.C. Yao, M. Huang, W. Li, H. Lu, X. Yuan, Y.B. Zhang, X. Jiang, C.Z. Peng and

- others, Observation of ten-photon entanglement using thin BiB 3 O 6 crystals. *Optica* **4**, 77–83 (2017).
- [58] P. Walther, M. Aspelmeyer and A. Zeilinger, Heralded generation of multiphoton entanglement. *Physical Review A* **75**, 012313 (2007).
- [59] X.L. Niu, Y.X. Gong, X.B. Zou, Y.F. Huang and G.C. Guo, Heralded multiphoton GHZ-type polarization entanglement generation from parametric down-conversion sources. *Journal of Modern Optics* **56**, 936–939 (2009).
- [60] C. Erven, E. Meyer-Scott, K. Fisher, J. Lavoie, B. Higgins, Z. Yan, C. Pugh, J.P. Bourgoin, R. Prevedel, L. Shalm and others, Experimental three-photon quantum nonlocality under strict locality conditions. *Nature Photonics* **8**, 292–296 (2014).
- [61] T.D. Ladd, F. Jelezko, R. Laflamme, Y. Nakamura, C. Monroe and J.L. O’Brien, Quantum computers. *Nature* **464**, 45–53 (2010).
- [62] J.L. O’Brien, A. Furusawa and J. Vučković, Photonic quantum technologies. *Nature Photonics* **3**, 687 (2009).
- [63] T. Rudolph, Why I am optimistic about the silicon-photon route to quantum computing. *APL Photonics* **2**, 030901 (2017).
- [64] F. Flamini, N. Spagnolo and F. Sciarrino, Photonic quantum information processing: a review. *Reports on Progress in Physics* **82**, 016001 (2018).
- [65] T.C. Ralph, N.K. Langford, T. Bell and A. White, Linear optical controlled-NOT gate in the coincidence basis. *Physical Review A* **65**, 062324 (2002).
- [66] J.L. O’Brien, G.J. Pryde, A.G. White, T.C. Ralph and D. Branning, Demonstration of an all-optical quantum controlled-NOT gate. *Nature* **426**, 264–267 (2003).
- [67] S. Gasparoni, J.W. Pan, P. Walther, T. Rudolph and A. Zeilinger, Realization of a photonic controlled-NOT gate sufficient for quantum computation. *Physical Review Letters* **93**, 020504 (2004).
- [68] N.K. Langford, T. Weinhold, R. Prevedel, K. Resch, A. Gilchrist, J. O’Brien, G. Pryde and A. White, Demonstration of a simple entangling optical gate and its use in Bell-state analysis. *Physical Review Letters* **95**, 210504 (2005).
- [69] A. Bocharov, M. Roetteler and K.M. Svore, Factoring with qutrits: Shor’s algorithm on ternary and meta-plectic quantum architectures. *Physical Review A* **96**, 012306 (2017).
- [70] M. Haghparast, R. Wille and A.T. Monfared, Towards quantum reversible ternary coded decimal adder. *Quantum Information Processing* **16**, 284 (2017).
- [71] M. Jafarzadeh, Y.D. Wu, Y.R. Sanders and B.C. Sanders, Randomized benchmarking for qudit Clifford gates. *arXiv:1911.08162* (2019).
- [72] X.L. Wang, X.D. Cai, Z.E. Su, M.C. Chen, D. Wu, L. Li, N.L. Liu, C.Y. Lu and J.W. Pan, Quantum teleportation of multiple degrees of freedom of a single photon. *Nature* **518**, 516–519 (2015).
- [73] X.M. Hu, C. Zhang, B.H. Liu, Y.F. Huang, C.F. Li and G.C. Guo, Experimental multi-level quantum teleportation. *arXiv:1904.12249* (2019).
- [74] X.M. Hu, W.B. Xing, C. Zhang, B.H. Liu, M. Pivovuska, M. Huber, Y.F. Huang, C.F. Li and G.C. Guo, Experimental creation of multi-photon high-dimensional layered quantum states. *arXiv preprint arXiv:2001.06253* (2020).
- [75] C. Parazzoli, B. Koltenbah, D. Gerwe, P. Idell, B. Gard, R. Birrittella, S. Rafsanjani, M. Mirhosseini, O. Magan-Loiza, J. Dowling and others, Enhanced Thermal Object Imaging by Photon Addition or Subtraction. *arXiv:1609.02780* (2016).
- [76] S.M.H. Rafsanjani, M. Mirhosseini, O.S. Magaña-Loaiza, B.T. Gard, R. Birrittella, B. Koltenbah, C. Parazzoli, B.A. Capron, C.C. Gerry, J.P. Dowling and others, Quantum-enhanced interferometry with weak thermal light. *Optica* **4**, 487–491 (2017).
- [77] L. Hardy, Source of photons with correlated polarizations and correlated directions. *Physics Letters A* **161**, 326–328 (1992).
- [78] P.G. Kwiat, K. Mattle, H. Weinfurter, A. Zeilinger, A.V. Sergienko and Y. Shih, New high-intensity source of polarization-entangled photon pairs. *Physical Review Letters* **75**, 4337 (1995).
- [79] X. Gu, L. Chen and M. Krenn, Quantum experiments and hypergraphs: Multiphoton sources for quantum interference, quantum computation, and quantum entanglement. *Physical Review A* **101**, 033816 (2020).
- [80] X. Zou, L.J. Wang and L. Mandel, Induced coherence and indistinguishability in optical interference. *Physical review letters* **67**, 318 (1991).
- [81] S.P. Walborn, C. Monken, S. Pádua and P.S. Ribeiro, Spatial correlations in parametric down-conversion. *Physics Reports* **495**, 87–139 (2010).

Supplementary Information:
**Conceptual understanding through
 efficient inverse-design of quantum optical experiments**
 Mario Krenn, Jakob Kottmann, Nora Tischler, Alán Aspuru-Guzik

I. BASIC ELEMENTS OF A GRAPH AS EXPERIMENTAL BUILDING BLOCKS

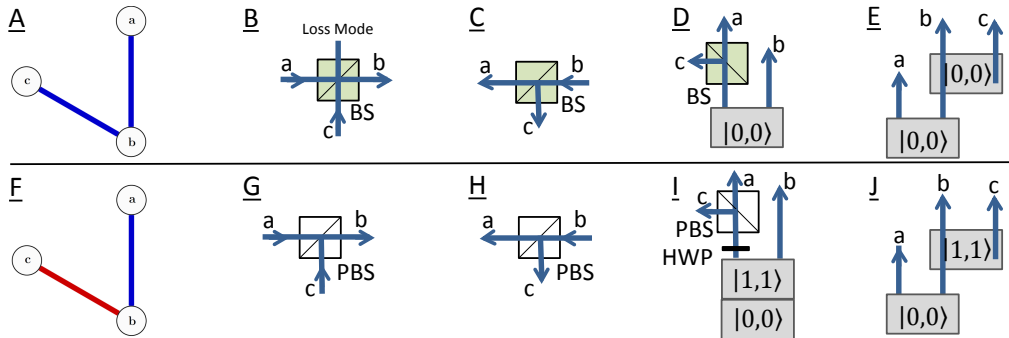


FigS. 6. Graph to experiment translation for individual edges.

Designing quantum optical experiments using the abstract notation of graphs is possible because we found translations of graphs into several different experimental schemes. Edges between vertices a and b are translated to probabilistic photon sources, see FigS.6A-F. Edge colours correspond to mode numbers. Multi-edges correspond to superposition or entanglement, and can be created with standard photonic technologies, for example, cross-crystal sources [77, 78]. A deterministic single-photon source emitting in path b can be understood as an edge between a vertex b and a virtual vertex V_a , FigS.6G. For each term in the resulting quantum state, every virtual vertices always need to have exactly one incoming edge. This is conceptually equivalent to the situation of a probabilistic photon-pair source, where the whole state is conditioned on the detection of one photon using a photon number sensitive detector in path V_a .

Edges can be merged at one vertex in several different ways, see FigS.7. If the edges have the same colour (FigS.7A), the corresponding photons have the same mode number. In that case, the edges can be merged with probabilistic beam splitters (green squares, FigS.7B-D) or by creating them directly with path identified photon-pair sources (for instance, SPDC crystals, FigS.7E).

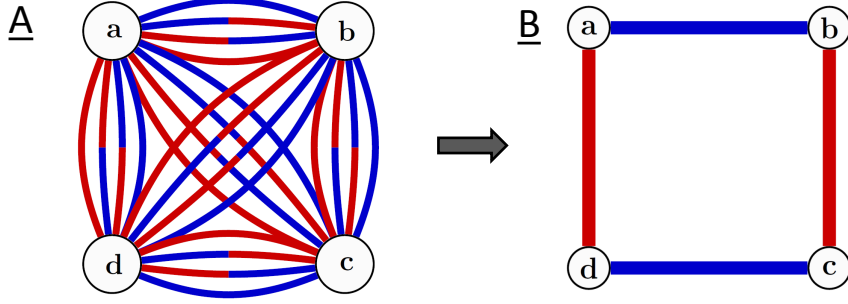
If the edges have different colour (FigS.7F), the corresponding photons have different mode numbers. In that case, the edges can be merged losslessly with mode-dependent beam splitters (so-called multiplexing or de-multiplexing); white squares, for example, polarizing beam splitters if the degree of freedom is photonic polarisation (FigS.7G-I). The edges could also be created by path identified photon-pair sources (for instance, SPDC crystals, FigS.7J). Other probabilistic photon sources, such as lasers as probabilistic single-photon sources, can be added by exploiting hypergraph structures [79].



FigS. 7. Graph to experiment translation. BS: beam splitter, PBS: polarizing beam splitter, HWP: half-wave plate

With the ability to create independent edges, and merge edges, all types of graphs can be translated to experimental setups. Appropriate phase shifters can manipulate the phases of edge weights. Additionally, amplitudes can be manipulated by pump power for SPDC crystals, splitting ratios that are set by half-wave plates, or absorptive filters. Collinear photon pair sources, that produce two photons in the same path, can be described with loops (an edge that connects a vertex to itself).

II. NORMALIZATION OF QUANTUM STATES



FigS. 8. **A:** A complete graph with four edges between each pair of vertices represents all possible correlations in a locally 2-dimensional system. **B:** In the optimization for a post-selected GHZ, it is reduced to a cycle graph.

We show how the state of a complete 2-coloured graph with four vertices can be written using the weight function $\Phi(\omega)$ of the graph in FigS.8A. It can be represented in terms of creation operators as

$$\Phi(\omega) \approx \sum_n \frac{1}{n!} \left(\sum_{\substack{x,y \in \{a,b,c,d\} \\ x < y}} \sum_{c_1, c_2 \in \{0,1\}} \omega_{x,y}^{c_1, c_2} x_{c_1}^\dagger y_{c_2}^\dagger + h.c. \right)^n. \quad (5)$$

If we are conditioning the state on one photon in each detector, it reduces to

$$|\psi\rangle = \frac{1}{N(\omega)} \sum_{i,j,k,l \in \{0,1\}} \omega_{|i,j,k,l\rangle} |i,j,k,l\rangle \quad (6)$$

with the edge weights

$$\omega_{|i,j,k,l\rangle} = \omega_{a,b}^{i,j} \cdot \omega_{c,d}^{k,l} + \omega_{a,c}^{i,k} \cdot \omega_{b,d}^{j,l} + \omega_{a,d}^{i,l} \cdot \omega_{b,c}^{j,k} \quad (7)$$

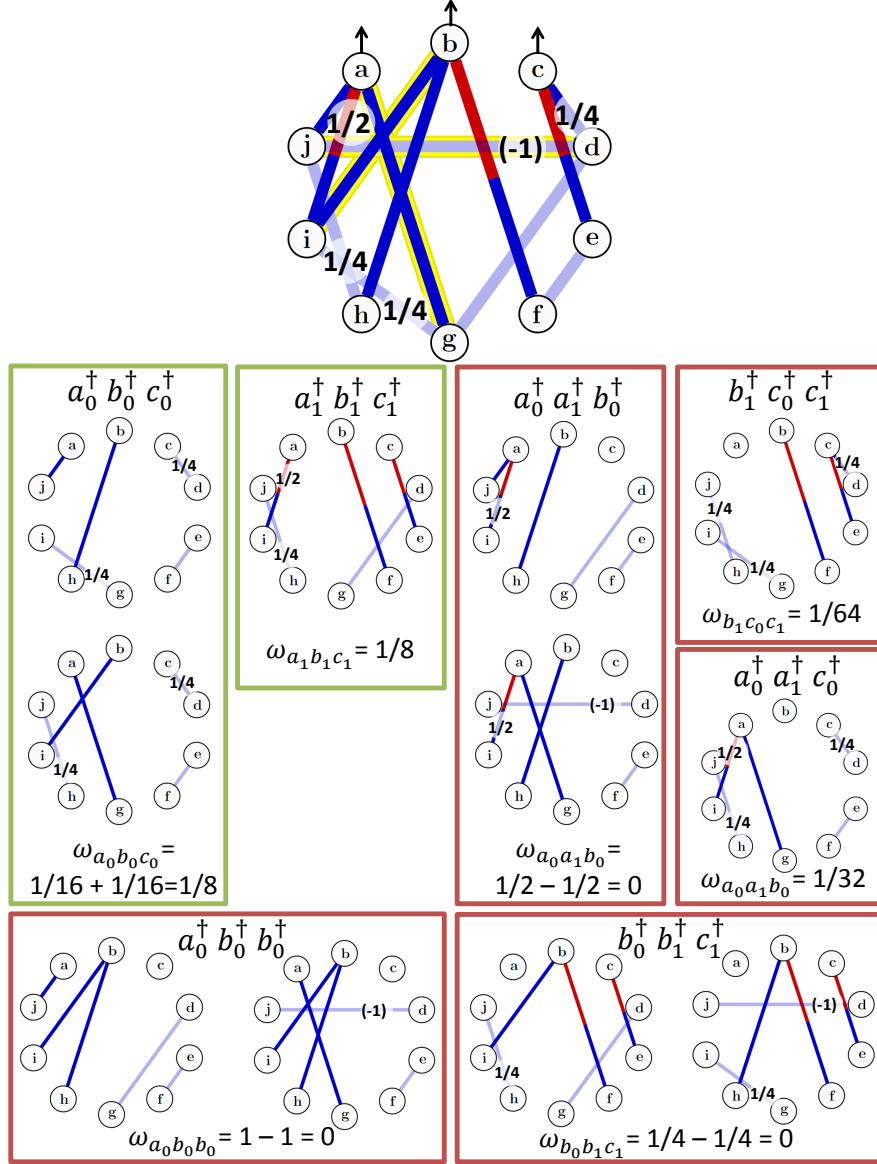
and the normalization constant

$$N(\omega) = \sqrt{\sum_{i,j,k,l \in \{0,1\}} |\omega_{|i,j,k,l\rangle}|^2}. \quad (8)$$

The objective of the optimization is to find $\omega_{x,y}^{i,j} \in \mathbb{C}$ that minimize the loss function, and subsequently finding solutions with a large number of edge weights being zero. The information about higher-order contributions to the state, which results in experimentally reduced quantum fidelities, is encoded within the weight function $\Phi(\omega)$. Therefore, higher-order contributions could be directly accounted for within the optimization procedure. More details about the approximations in eq.(5) can be found in [80, 81].

III. HERALDED GHZ STATE

In FigS.9, we show the individual terms contributing to a heralded GHZ state. For the optimization, we started with a complete graph with seven heralding detectors, whose simultaneous photon clicks lead to a GHZ

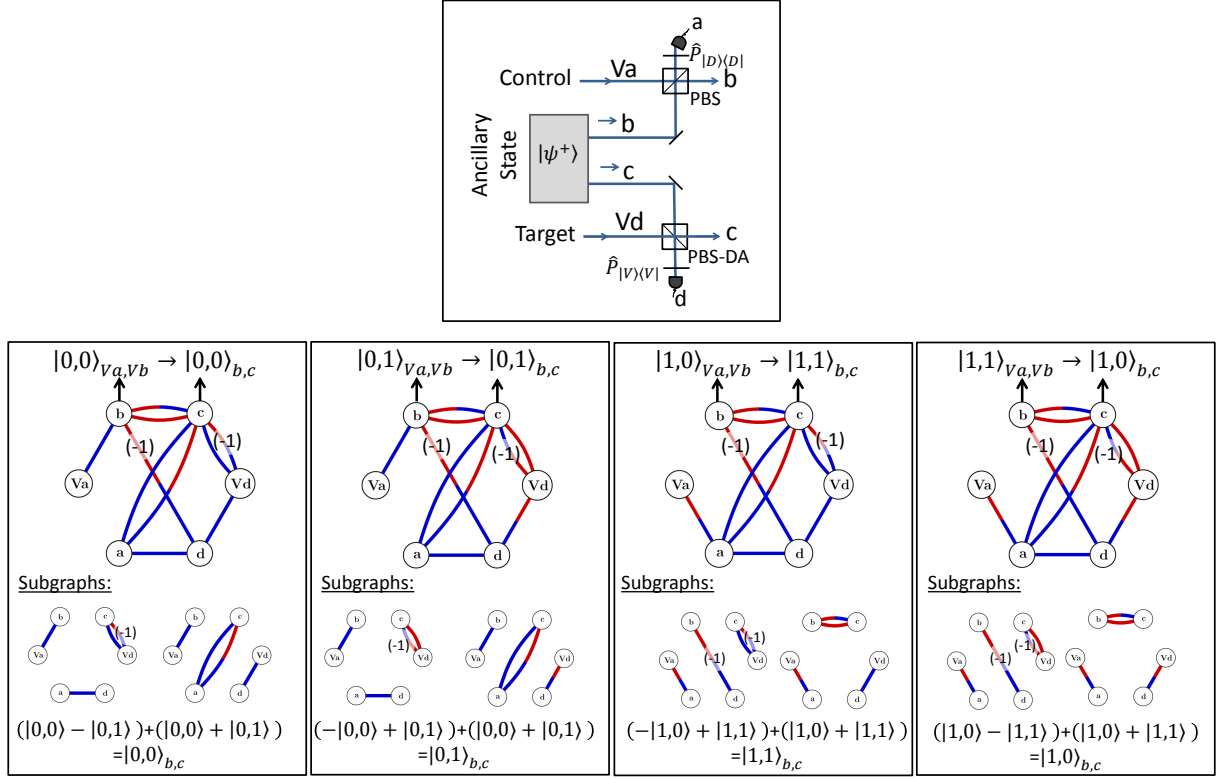


FigS. 9. Heralded GHZ State.

state in the paths a, b, c . For that reason, the resulting solution is a 10-photon experiment. It is not necessary to know the number of required ancillary detectors before the optimization. Instead, one could start with even larger graphs. As a result, the topological optimization will reduce the number of unnecessary edges. The topological optimization will reveal whether an unnecessarily large number of ancillary detectors has been provided. In that case, a pair of vertices will be connected only to itself and not to other vertices in the graph. This pair of vertices can then be safely removed from the final graph.

If all heralding detectors simultaneously detect a photon in state $|0\rangle$, then the output in paths a, b, c is in the state $|\psi\rangle \approx 1/\sqrt{2}(|0, 0, 0\rangle + |1, 1, 1\rangle)$. The saturation of the colours in FigS.9 reflects the magnitude of the associated weights so that the weight of edges in light blue are significantly smaller (by a factor $s \ll 1$) than the edges in strong blue. The optimization resulted in small weights on the four edges between the triggers which diminishes the probability to have those triggers active without having a valid GHZ state in a, b, c .

If we use the strategy that worked for arbitrary high-dimensional heralded Bell states, we have to connect each edge from a, b, c to one individual vertex. The upper graph represents this case without the three yellow marked edges. In that case, however, four terms are generated, which correspond to the four subgraphs in the first row. They involve the two GHZ-terms, but also two other terms that do not correspond to the GHZ, which significantly reduces the fidelity.



FigS. 10. 2-dimensional CNOT gate, performed by Gasparoni et al.,[67].

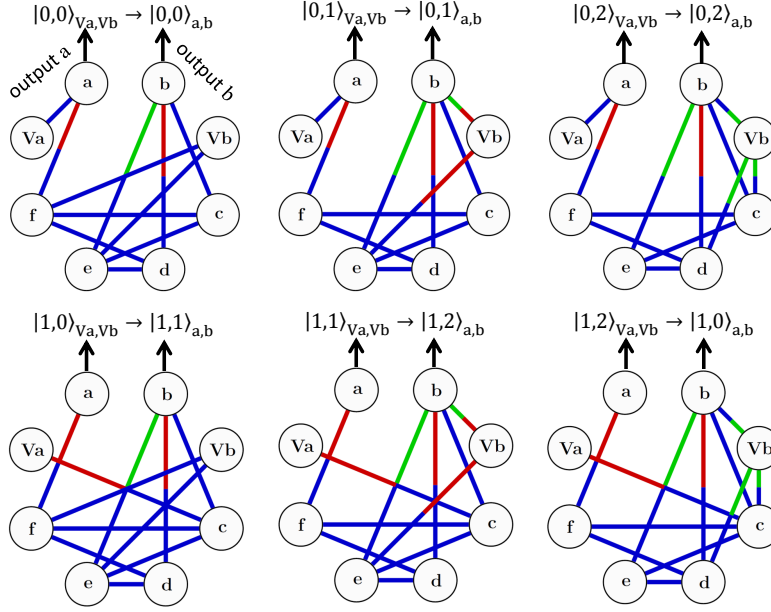
The algorithm THESEUS finds an extension of the original idea to increase the fidelity. Keep in mind that the coefficients of a specific term are the sum of all subgraph weights leading to that term, and the weight of a subgraph is the product of all edge weights.

THESEUS adds three extra edges to the graph (marked in yellow), which have two independent effects: First, it adds the edge $a-g$ and the negatively weighted edge $d-j$ in such a way that it can destructively interfere one of the undesired terms. Second, it adds one additional edge between $b-i$, which leads to a second subgraph that corresponds to $|0,0,0\rangle$ (first graph in the second row, within the green box). As the weights of $|0,0,0\rangle$ and $|1,1,1\rangle$ need to be the same, two graphs corresponding to one term give the additional freedom that is necessary to reduce the weight of the fourth term (last graph in the first line) to a small value. Thereby, the final fidelity is close to one. In this example, to simplify explanations and understanding, we restrict ourselves to coefficients of 1, 1/2 and 1/4. Access to other coefficients leads to fidelities arbitrarily close to one. The final state can be written as

$$|\psi\rangle = N \cdot \left(\underbrace{\frac{1}{8} (|0,0,0\rangle + |1,1,1\rangle)_{a,b,c}}_{\text{GHZ state}} + \underbrace{\frac{1}{64} (2\hat{a}_0^\dagger \hat{a}_1^\dagger \hat{b}_0^\dagger |vac\rangle + \hat{b}_1^\dagger \hat{c}_0^\dagger \hat{c}_1^\dagger |vac\rangle)}_{\text{noise terms}} + \underbrace{\mathcal{O}(s)}_{\text{more than 2 edges between ancillary detectors}} \right) \quad (9)$$

with the normalization $N = \sqrt{\frac{4096}{133}}$, and $|vac\rangle$ standing for the vacuum state. The fidelity is larger than 96%. This example shows how topological optimization (and restrictions of coefficients to small rational numbers) helps to understand the conceptual core of the solution. From the solution, we can not only interpret how the heralded GHZ is generated, but can understand the idea of destructive interference (via adding a negatively weighted edge), and increasing the flexibility of edge weights by having two subgraphs corresponding to one term.

More than ten years ago, schemes for heralded GHZ states have been proposed [58, 59], which require experimentally significantly more resources and have therefore not yet become practical. In particular, the



FigS. 11. High-dimensional CNOT gate, with a qubit control photon and a qutrit target photon.

3-photon GHZ proposal by Walther et al. [58, 59] requires 12 photons (nine ancillary photons that herald a GHZ state). The proposal by Niu et al., [59] requires ten photons (seven ancillary photons), but further requires close to perfectly efficient, photon-number-sensitive detectors for heralding paths, as they need to distinguish between the arrival of one and two photons. In contrast, our proposal requires only ten photons and non-photon number resolving detectors – which is feasible in state-of-the-art photonic laboratories.

IV. EXPERIMENTAL 2-QUBIT CNOT

A photonic CNOT transformation was performed by Gasparoni et al., [67] in 2004, which can be seen in FigS.10. An ancillary state $|\psi^+\rangle = 1/\sqrt{2}(|0,1\rangle + |1,0\rangle)$ in paths b and c is combined with the incoming control and target photons. A simultaneous detection event in detector a and d heralds a successful realization of a CNOT.

The corresponding graphs for the four different cases are seen below. The resulting states correspond to all subgraphs with one incoming edge in vertex a and one in vertex d (those are heralding detectors), and one edge from each vertex Va and Vd (those represent the incoming photons). It can be seen that Vd (which corresponds to the incoming photon from path d , i.e. the target photon) is responsible for the phase of the quantum states. In that way, it is responsible for the term that is destructively interfered – this is analogous to the situation presented in the main text.

V. CNOT BEYOND QUBITS

A control operation in a 2×3 dimensional space is shown in FigS.11. The subgraph $a-f$ remains constant, while the edges containing Va and Vb changes depending on the input control/target photons. The correct transformation is heralded by simultaneous detection of a photon in each of the detectors $c-f$.

The structure of the subgraph $a-f$ is very reminiscent of the solution of heralded Bell states in Fig.3 of the main text. Here, each internal mode (represented as edge colour) from a and b is connected to one individual heralding detector.

Furthermore, the solution uses destructive interference for producing the correct output states, as in Fig.4 of the main text. Some of the resulting subgraphs (those have one incoming edge to vertex $c-f$) do not vanish. Still, they are reduced in magnitude by adapting the edge weights appropriately, in an analogous way, as shown in FigS.9. Thereby, an experimentally feasible method of performing CNOT transformations beyond qubits is constructed.